

---

# DECISION-DIRECTED DATA DECOMPOSITION

---

A PREPRINT

Brent D. Davis<sup>\*1</sup>, Ethan Jackson<sup>1,2</sup>, and Daniel J. Lizotte<sup>1,3</sup>

<sup>1</sup>Department of Computer Science, The University of Western Ontario, London, ON N6A 5B7, Canada

<sup>2</sup>Vector Institute, Toronto, ON M5G 1M1, Canada

<sup>3</sup>Department of Biostatistics & Epidemiology, Schulich School of Medicine and Dentistry, The University of Western Ontario, London, ON N6A 5C1, Canada

April 26, 2022

\*Corresponding author

## ABSTRACT

We present an algorithm, Decision-Directed Data Decomposition, which decomposes a dataset into two components. The first contains most of the useful information for a specified supervised learning task, and the second orthogonal component that contains little information about the task. The algorithm is simple and scalable. It can use kernel techniques to help preserve desirable information in the decomposition. We illustrate its application to tasks in two domains, using distributed representations of words and images, and we report state-of-the-art results showcasing  $D_4$ 's capability to remove information pertaining to gender from word embeddings.

## 1 Introduction

Distributed feature representations of complex entities are useful for many tasks. For example, word embeddings are used both for supervised learning tasks and for data exploration and sense-making tasks in a variety of domains [Dai et al., 2017]. Image representations from deep learning models have also found many uses outside of the task they were originally trained on [Gatys et al., 2016]. However, such representations can carry information that is undesirable, either because it reflects undesirable bias (e.g. gender bias in word embeddings [Caliskan et al., 2017]) or because it obfuscates other information that is relevant to the task at hand [Ribeiro et al., 2016], which can impact both data exploration and ability to generalize.

We introduce Data-Directed Data Decomposition ( $D_4$ ), a technique to decompose a data matrix into two components. One component contains information about a specified classification or regression target that a linear model can use for prediction, and the other that does not contain such information. It is this second component, orthogonal to the first, that is useful for further analyses that should exclude information about the specified target, as we will demonstrate.

For this work, our ultimate goal is to support data exploration and sense-making tasks that seek to understand relationships between objects in a dataset (e.g. words, documents), rather than to develop a predictive model that will be applied to future data; hence we focus our attention on  $D_4$ 's ability to remove information and bias in this setting. That said, there is also the potential for  $D_4$  to be applied in predictive settings as well. We consider applications that would normally be served by adversarial learning, where it is important to remove the ability to learn certain concepts from a representation, often to promote better generalization [Biggio et al., 2014]. Hence, we explore this setting as well.

We describe our algorithm in detail in Section 2. We identify uses of  $D_4$  and provide illustrative experimental examples in Section 3, including state-of-the-art results on word embedding de-biasing. Our work is related to and builds upon a large body of work in the geometric interpretation and manipulation of data; in Section 4 we discuss connections to these related methods and formalize additional properties of  $D_4$  to describe the connections. Finally in Section 5 we conclude and identify future directions of research.

## 2 Decision-Directed Data Decomposition

Our approach uses generalized linear supervised learning methods whose decision functions are of the form  $h(\mathbf{x}) = g(\mathbf{x}^\top \mathbf{w})$ , where  $\mathbf{w}$  is learned from labelled data and represents a direction in feature space that is most useful for predicting a target  $\mathbf{y}$ , according to the loss function of the learner. (E.g. cross-entropy for logistic regression, hinge for SVM, and so on.) Our approach is to find these most useful directions and then project the data onto their orthogonal complement to create a new dataset with which we are *not* able to fit the target well. The resulting data can then be used subsequently for analyses where learners should *not* make use of the target concepts—whether explicitly or implicitly—in order to label future instances. We begin by presenting a simple example of how this works, followed by the complete  $D_4$  algorithm applicable to  $n \times p$  feature matrices; a version applicable to  $n \times n$  kernel matrices is provided in the supplemental material.

For a  $p \times 1$  unit vector  $\boldsymbol{\omega}$ , the projection of the rows of a matrix  $\mathbf{X}$  onto  $\boldsymbol{\omega}$  is given by  $\mathbf{X}_{\parallel} = \mathbf{X}\boldsymbol{\omega}\boldsymbol{\omega}^\top$ , and the projection onto its orthogonal complement is given by  $\mathbf{X}_{\perp} = \mathbf{X}(\mathbf{I} - \boldsymbol{\omega}\boldsymbol{\omega}^\top)$ .

$$\text{For example, if } \mathbf{X} = \begin{bmatrix} 1 & 0 & 1 \\ 0 & 1 & 1 \\ 1 & 0 & 0 \\ 0 & 1 & 0 \end{bmatrix} \text{ and } \boldsymbol{\omega} = \begin{bmatrix} 0 \\ 0 \\ 1 \end{bmatrix}, \text{ then } \mathbf{X}_{\parallel} = \begin{bmatrix} 0 & 0 & 1 \\ 0 & 0 & 1 \\ 0 & 0 & 0 \\ 0 & 0 & 0 \end{bmatrix} \text{ and } \mathbf{X}_{\perp} = \begin{bmatrix} 1 & 0 & 0 \\ 0 & 1 & 0 \\ 1 & 0 & 0 \\ 0 & 1 & 0 \end{bmatrix}.$$

Note that  $\mathbf{X} = \mathbf{X}_{\parallel} + \mathbf{X}_{\perp}$ ,  $\mathbf{X}_{\parallel}\mathbf{X}_{\perp}^\top = \mathbf{X}_{\perp}\mathbf{X}_{\parallel}^\top = \mathbf{0}$ , and  $\mathbf{X}_{\perp}\boldsymbol{\omega} = \mathbf{0}$ ; hence if we consider the rows of  $\mathbf{X}_{\perp}$  as points in  $\mathbb{R}^3$ , they have zero variability in the direction of  $\boldsymbol{\omega}$ ; in other words, all information about where the points lie in the direction of  $\boldsymbol{\omega}$  has been removed and therefore  $\mathbf{X}_{\perp}$  could be used in future analyses where that direction should be excluded from decision-making.

In practice, it is unlikely that in a distributed representation only one direction contains information about a given target. Hence, we propose to take the  $\mathbf{X}_{\perp}$  resulting from the first projection and remove the next best decision-direction, resulting in a new  $\mathbf{X}_{\perp}$ , and so on. If we continue this process, eventually we will have  $\mathbf{X}_{\parallel} = \mathbf{X}$  and  $\mathbf{X}_{\perp} = \mathbf{0}$ , which obviously contains no information about the target (or about anything else). At any step along the way, we have removed some of the information about  $\mathbf{y}$  from  $\mathbf{X}$  that can be recovered by (generalized) linear learners, and in practice the quantity that remains can be reduced essentially to zero. We next describe this process in detail in the context of an explicit feature representation; a version operating on the implicit feature representation defined by a kernel is provided in the supplemental material.

We now present the complete  $D_4$  algorithm as it applies to a data matrix of examples with explicitly defined features. Let  $\mathbf{X}$  be an  $n \times p$  matrix of feature vectors, each of length  $p$ , and let  $\mathbf{y}$  be an  $n \times 1$  vector of supervised learning targets. Let  $\mathbf{w}$  be a  $p \times 1$  decision vector learned from  $\mathbf{X}$  and  $\mathbf{y}$ , and let  $\boldsymbol{\omega} = \mathbf{w}/\|\mathbf{w}\|$ . The projection of the rows of  $\mathbf{X}$  onto the space orthogonal to  $\boldsymbol{\omega}$  is given by  $\mathbf{X}_{\perp} = \mathbf{X}(\mathbf{I} - \boldsymbol{\omega}\boldsymbol{\omega}^\top)$ . For all feature vectors  $\mathbf{x}_{\perp i}$   $i \in 1..n$  which correspond to the rows of  $\mathbf{X}_{\perp}$ , we have  $\mathbf{x}_{\perp i}^\top \boldsymbol{\omega} = 0$ . We note the following simplification that can be made when performing sequential orthogonal projections.

**Lemma 1** (Orthogonal projections - explicit features). *If for all  $\boldsymbol{\omega}^{(i)}, \boldsymbol{\omega}^{(j)}$  in  $\boldsymbol{\omega}^{(1)}, \boldsymbol{\omega}^{(2)}, \dots, \boldsymbol{\omega}^{(p)}$  we have  $\boldsymbol{\omega}^{(i)\top} \boldsymbol{\omega}^{(j)} = 0$ , then  $\mathbf{X} \prod_i (\mathbf{I} - \boldsymbol{\omega}^{(i)} \boldsymbol{\omega}^{(i)\top}) = \mathbf{X}(\mathbf{I} - \sum_i \boldsymbol{\omega}^{(i)} \boldsymbol{\omega}^{(i)\top})$ .*

Using this lemma, we define  $\boldsymbol{\Omega}^{(i)} \leftarrow \mathbf{I} - \sum_{j=1}^i \boldsymbol{\omega}^{(j)} \boldsymbol{\omega}^{(j)\top}$ , which is the projection onto the space orthogonal to all of  $\boldsymbol{\omega}^{(1)}$  through  $\boldsymbol{\omega}^{(i)}$ . This allows us to define  $\mathbf{X}_{\perp}^{(i)} = \mathbf{X}\boldsymbol{\Omega}^{(i)}$  and  $\mathbf{X}_{\parallel}^{(i)} = \mathbf{X} - \mathbf{X}_{\perp}^{(i)}$ . Our learner can then use  $\mathbf{X}_{\perp}^{(i)}$  and  $\mathbf{y}$  to identify the next direction to remove, and so on.

Note that the rank of  $\boldsymbol{\Omega}^{(i)}$  is  $p - i$ , and the rank of  $\mathbf{X}_{\perp}^{(i)}$  is also  $p - i$  assuming  $\mathbf{X}$  had full rank to begin with. If the learning algorithm to be used with  $D_4$  requires a full-rank feature matrix, we can use Gram-Schmidt orthogonalization to produce an equivalent full-rank representation as follows. Create a matrix  $\mathbf{G} = [\boldsymbol{\omega}^{(1)}, \dots, \boldsymbol{\omega}^{(i)} | \boldsymbol{\psi}^{(i+1)}, \dots, \boldsymbol{\psi}^p]$ , choosing the  $\boldsymbol{\psi}$  so that  $\mathbf{G}$  has full rank<sup>1</sup>. Perform (possibly modified) Gram-Schmidt orthogonalization<sup>2</sup> on  $\mathbf{G}$ . Since the  $\boldsymbol{\omega}^{(1)}, \dots, \boldsymbol{\omega}^{(i)}$  are already orthonormal they will be left alone, and the remaining columns will form an orthonormal basis for their orthogonal complement; call those columns  $\mathbf{P}_{\Omega}$ . The learner can then use  $\mathbf{X}\mathbf{P}_{\Omega}$  and  $\mathbf{y}$  to learn the next direction  $\tilde{\mathbf{w}}$  in  $p - i$  dimensions, and then project that weight vector up to  $p$  dimensions to obtain  $\mathbf{w} = \mathbf{P}_{\Omega}^\top \tilde{\mathbf{w}}$ . Even if

<sup>1</sup>If for example they are drawn from a continuous distribution this will be the case almost surely.

<sup>2</sup>This can be achieved e.g. by QR-decomposition, for which there are many very good implementations.

the learner does not require a full-rank input, the orthogonalization process may be desirable for numerical stability with large  $p$ . This process is detailed in Algorithm 1.

**Data:** Feature matrix  $\mathbf{X}$  ( $n \times p$ ) of training points, targets  $\mathbf{y}$  ( $n \times 1$ ).

**Result:** Orthogonal basis vectors  $\omega^{(1)}, \omega^{(2)}, \dots, \omega^{(p)}$

**for**  $i$  from 1 to  $p$  **do**

**if** learner does not require a full-rank feature matrix **then**

$\Omega \leftarrow \mathbf{I} - \sum_{j=1}^{i-1} \omega^{(j)} \omega^{(j)\top}$ ;

$\mathbf{w} \leftarrow \text{learn}(\mathbf{X}\Omega, \mathbf{y})$ ;

**else**

$(\mathbf{Q}_\Omega, \mathbf{R}_\Omega) \leftarrow \text{qr.decomposition}([\omega^{(1)}, \dots, \omega^{(i-1)} | \psi^{(i)}, \dots, \psi^p])$ ;

$\mathbf{P}_\Omega \leftarrow$  last  $p - i$  columns of  $\mathbf{Q}_\Omega$ ;

$\tilde{\mathbf{w}} \leftarrow \text{learn}(\mathbf{X}\mathbf{P}_\Omega, \mathbf{y})$ ;

$\mathbf{w} \leftarrow \mathbf{P}_\Omega^\top \tilde{\mathbf{w}}$ ;

**end**

$\omega^{(i)} \leftarrow \mathbf{w} / \|\mathbf{w}\|$ ;

**end**

**Algorithm 1:**  $D_4$  Algorithm - Feature Representation

If the learner does not require a full-rank feature matrix, then the time cost per iteration is  $\mathcal{O}(p^2)$  to form  $\Omega$  (if it is updated in-place from the previous iteration) and  $\mathcal{O}(np^2)$  to project  $X$ , plus the cost of learning. If the learner requires a full-rank feature matrix, then the time cost per iteration is  $\mathcal{O}(p^3)$  to form  $\mathbf{P}_\Omega$  by Gram-Schmidt or QR and  $\mathcal{O}(n(p-i)p)$  to project  $X$ , plus the cost of learning. In both cases, the space complexity (additional to storage of  $\mathbf{X}$  and  $\mathbf{y}$ ) is  $\mathcal{O}(p^2)$  to store the  $\omega^{(i)}$ .

### 3 Application Examples

We now present three examples of how  $D_4$  can be applied. First we show using an image processing example that  $D_4$  is able to remove information about a specified target concept without interfering with other important tasks. Next, we use an example to show when and how  $D_4$  can lead to improved generalization in supervised learning. Finally, we show how  $D_4$  can be used for de-biasing of word embeddings, providing state-of-the-art results. Experiments were run on a Windows 10 Professional PC with an i9-7900X CPU (10 real / 20 virtual cores @3.33GHz), 64GB of DDR4 RAM and 3TB hard drive. Source code will be made available at [www.github.com/bdavis56/DDDD](http://www.github.com/bdavis56/DDDD)

#### 3.1 Target Concept Removal

Our first example demonstrates that  $D_4$  can remove information about one target without sacrificing accuracy on other targets—even those that are related. We applied  $D_4$  to representations of images in the feature space induced by the second-to-last layer of a VGG19 deep convolutional image classification model [Simonyan and Zisserman, 2014] pre-trained on ImageNet. An independently-collected test set of ImageNet class images [Recht et al., 2019] provided 7000 images evenly distributed over 700 classes. Of these, 350 classes each correspond to animate and inanimate objects, which we used to create an additional set of class labels. We used the pre-trained VGG19 model to transform each image to a 4096-dimensional representation space in which  $D_4$  was applied in an effort to remove the target concept of (in)animacy without impacting accuracy.

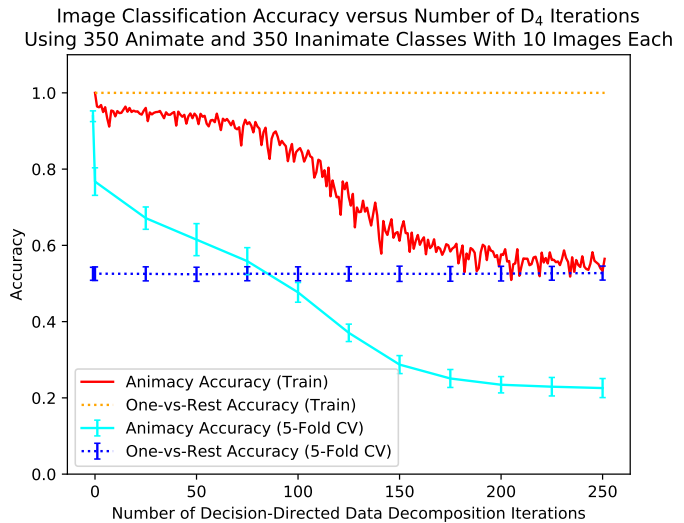


Figure 1: Accuracy on two tasks: classifying animacy versus inanimacy, and object category labelling, as a function of iterations of  $D_4$ .

Results are summarized in Figure 1. The solid lines show the training and CV accuracy on the binary classification task of telling whether the object is animate or inanimate. This is the specified target that  $D_4$  uses to project the data. The dotted lines indicate accuracy on the 700-class classification problem of image categorization. For both tasks, training accuracy and 5-fold cross validation accuracy are shown. First, we note that our goal was not to demonstrate state-of-the-art ImageNet performance, and that no tuning of the classifiers was undertaken; in both cases a linear SVM with  $C = 1$  was used, with the usual binary formulation for the animacy problem and a one-versus-all formulation for the image categorization problem. Nonetheless, CV accuracy for animacy before  $D_4$  was approximately 0.94 (baseline 0.5) and for the image categorization was 0.53 (baseline  $1/700 = 0.0014$ ). This good performance is a testament to the representation previously learned by the neural network.

The CV accuracy of the animacy task drops drastically from 0.94 to 0.74 after the first projection step, after which it slowly decreases, crossing baseline accuracy after about 100 projections. It then continues to fall to performance worse than random as more dimensions are removed. The training accuracy follows a similar trajectory; we believe the “noisy” component of the training error is due to numerical stability issues and might be rectified by allowing the SVM learning algorithm more time to converge; nonetheless we confirmed that the classifiers being learned are mutually orthogonal.

There is essentially no change in the training or CV error of the one-versus-all image categorization task, even as the ability to distinguish animacy from inanimacy tends to zero. This may seem counter-intuitive since the image classes partition the animate and inanimate categories; however a simple example may help explain what is happening. Consider the following dataset with two features and a label:  $(1, 0, a), (0, 1, b), (-1, 0, A), (0, -1, B)$ . In this example, if we ignore case, the  $(A/a)$ s are not linearly separable from the  $(B/b)$ s (this is essentially the classic XOR setting.) However, each of the four distinct labels is linearly separable from all of the others. This experiment shows that  $D_4$  is able to find a representation that “mixes” the animate and inanimate objects while preserving their original separability, without knowing what the individual classes are.

### 3.2 Improving Generalization

Our second example illustrates how the application of  $D_4$  can improve generalization error in particular settings by enforcing invariants. It has been long established that in order to achieve generalizability, predictive models must be invariant to features or concepts that are correlated with the specified target in the training set but that may be uncorrelated or even anti-correlated in other settings. As an extreme example, Ribeiro et al. [2016] constructed a synthetic setting where a classifier is trained to distinguish images of wolves from images of huskies, but where the wolves are only shown in snow and the huskies are never shown in snow. The resulting classifier is able to achieve 100% training accuracy, but has no ability to generalize when presented with huskies in snow or wolves not in snow because its predictions are driven entirely by the presence of snow in the image.

We create a prototypical example to both illustrate this effect and demonstrate how  $D_4$  can mitigate it. R code [Team et al., 2013] for this simulation is supplied in the supplemental material. Consider a dataset with  $n = 100000$  and  $p = 300$ . We generate two random orthogonal directions,  $w_1^*$  and  $w_2^*$ , in this space, which define two targets  $y_1(x) = \varepsilon \text{sgn } x^\top w_1^*$  and  $y_2(x) = \varepsilon \text{sgn } x^\top w_2^*$ , where  $P(\varepsilon = 1) = 0.9$  and  $P(\varepsilon = -1) = 0.1$ . We generate  $n = 100000$  multivariate normal feature vectors such that the correlation between  $x^\top w_1^*$  and  $x^\top w_2^*$  is 0.9 and the standard deviations of  $x^\top w_1^*$  and  $x^\top w_2^*$  are 1 and 2, respectively, then we generate the labels  $y_1$  and  $y_2$ . This effectively makes the signal in  $w_2^*$  “stronger” than that in  $w_1^*$  for linear classifiers that have a prior that prefers small weights, i.e. that are regularized. We generate a test set that is the same in all respects except that the correlation is  $-0.9$ .

First, we train ridge logistic regression classifiers with  $\lambda = 1$  on both  $y_1$  and  $y_2$ . This achieves good training error for both, and good test error for  $y_2$ , but very poor test error for  $y_1$ . This is because the classifier for  $y_1$  is mostly using  $w_2^*$  to discriminate; in the training data both  $w_1^*$  and  $w_2^*$  are good for discriminating  $y_1$ , but this is not the case in the test data where the correlation has been reversed. After we apply one iteration of  $D_4$  and use the resulting data to train new classifiers, the test accuracy for  $y_1$  jumps from 0.26 to 0.82, while the test accuracy for  $y_2$  falls from 0.87 to 0.27. It is worth noting that the training error for  $y_1$  actually falls from 0.81 to 0.61, as removal of the  $w_2^*$  component makes fitting the regularized logistic regression more difficult, despite the improved test error. Table 1 summarizes the results, and also shows the loadings of weight vectors of each classifier onto  $w_1^*$  and  $w_2^*$ , to illustrate which directions the classifiers are making use of.

### 3.3 De-biasing

Our third example demonstrates how target concept removal can be applied to concepts like gender in the setting of de-biasing. Recent work has reignited interest in de-biasing word embeddings by showing that not all the analogies that can be generated with word embeddings are desirable. Man - King + Woman = Queen was an exciting result, but Man - Programmer + Woman = Homemaker was not [Bolukbasi et al., 2016]. We refer to Bolukbasi et al.’s approach

Table 1: Performance on task defined by  $\mathbf{y}_1$  before and after using  $D_4$  to remove information about the task defined by  $\mathbf{y}_2$ . “Iteration 0” refers to classifiers constructed using the original data. Iteration 1 shows results after one iteration of  $D_4$ . “Loadings” give the dot product between the learned classifier weights (normalized) and the weight vector used to define the decision boundary.

Iteration	Target	Train Accuracy	Test Accuracy	Weight on $w_1^*$	Weight on $w_2^*$
0	$\mathbf{y}_1$	0.81	0.26	0.54	1.68
	$\mathbf{y}_2$	0.88	0.87	0.39	1.83
1	$\mathbf{y}_1$	0.61	0.82	0.84	-0.69
	$\mathbf{y}_2$	0.52	0.27	0.64	-0.48

hereafter as HARD-DEBIAS. This approach was followed by a way to learn gender neutrality at the time of training, named GN-GloVe, by Zhao et al. [2018]. This approach describes a way to try to contain all gender information to a specific space within their embedding that can later be discarded.

Both approaches are successful in mitigating some bias while preserving the functional aspects of the word embeddings. However, close examination of more ingrained problematic biases by Gonen and Goldberg [2019] (henceforth referred to as GG) revealed that while the de-biasing is effective for the exact target concepts it was meant to remove, those concepts can still be recovered by other methods. We task  $D_4$  to more deeply dis-entrench gender information from word embeddings. We provide Python code in the supplemental material which can apply  $D_4$  to word embeddings. We use both scikit-learn [Pedregosa et al., 2011] and SciPy [Jones et al., 2014].

Our approach builds on HARD-DEBIAS’s definition of a subspace using pre-selected *instances*, where an instance is a pair of words and their corresponding embedded representations. Each selected pair, for example *her*, *his*, or *she*, *he*, defines a direction in the representation space. HARD-DEBIAS takes these directions, summarizes them using PCA to find a single predominant “gender direction,” and then projects representations onto this orthogonal complement. All words not used in the gender direction are set to be zero on the gender direction. To replicate the work by GG, we take the gender direction to be the difference between *he* and *she*.

We borrow the notion of gender directions but instead apply  $D_4$  to find decision directions that separate vectors of male- and female-labeled words, using the list of male and female words of Zhao et al. [2018]. We then project all words in the embedding orthogonal to the resulting directions.

In order to determine the number of projections to perform, we measure the training and CV accuracy at each projection of  $D_4$  for predicting gender direction. Using a linear SVM, we observed gender direction accuracy to level off at 0.591 after 6 projections. Further projections do not change the training accuracy. We use this as the end point of our decomposition. We project 2, 4 and 6 times and measure clustering after each. Further, we provide a proof-of-principle run of 300 projections that completely removes all information aside from magnitude. Magnitude can be interpreted as word frequency in this setting and is visualized with a word cloud (Appendix Figure 1).

GG noticed that the most positive and negative words on the gender direction cluster together from k-means, and this clustering persists through de-biasing. We reproduce the gender direction vector using the w2vnews embedding set provided with HARD-DEBIAS. We use k-means,  $k=2$  to cluster the 500 most biased words from each extreme of the gender direction into two clusters. Matching gender labels to clusters is 99.8% accurate on w2vnews and 99.98% accurate on full Google News. This accuracy is used to measure ‘bias by neighbour’ by GG. GG observed clustering matching gender label in 92.5% cases after HARD-DEBIAS and 85.6% of cases in GN-GloVe. Projections 2, 4 and 6 achieve reductions of clustering accuracy to 95.9%, 87.4% and 74.3% on w2vnews.

We use T-SNE (2 components, perplexity 40, 300 iterations) [Van Der Maaten and Hinton, 2008] to visualize the gender vectors before and after 6 projections (Figure 2). We observe migration of some vectors across previous ‘class divisions’ in Figure 2, which visually suggests that  $D_4$  is successfully projecting vectors in a way that diminishes bias by neighbours phenomenon. T-SNE plots for 2&4  $D_4$  projections are appended (Appendix Figures 2&3). Word clouds showing changes in words on the female gender direction before and after the 6th  $D_4$  projection are in Appendix Figures 4&5.

As we are using clustering to ‘classify’, we also report the v-measure scores [Rosenberg and Hirschberg, 2007] ( $\beta = 1$ ) of 0.9896 for w2vnews and 0.9896 for Google News. This measures the completeness — the degree to which all class elements are member of the same cluster or not, and homogeneity — the degree to which all clusters contain only data points which belong to a single class. A score of 1.0 indicates perfect clustering and decreasing scores indicate decreasing quality. The v measure scores ( $\beta = 1$ ) for  $D_4$  projections 2, 4 and 6 are 0.7682, 0.4852 and 0.1794 respectively. This shows a loss in ability to cluster by gender label, and the corresponding v-scores show that the cluster coherency falls as the number of projections increases.

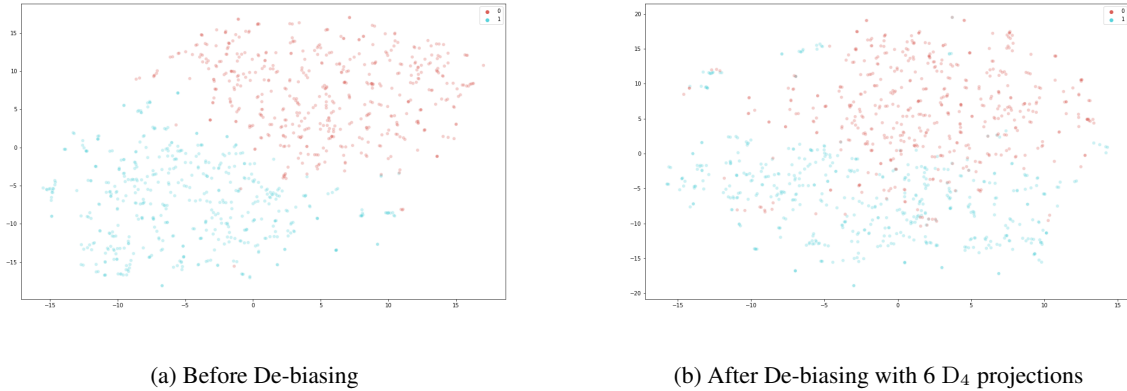


Figure 2: Visualization of gendered word vectors before and after  $D_4$  using T-SNE. Vectors are coloured by gender (female  $\rightarrow$  red, male  $\rightarrow$  blue).

We then apply our technique to the full Google News embedding to test on a larger set.  $D_4$  projections of 2, 4 and 6 yield accuracies of 71.6%, 67.4% and 68.2%, respectively. Training accuracy does not level off after 6 projections here. Future work could explore a more detailed decomposition of this set. Appendix Figures 6–9 visualize T-SNE clusters for the raw vectors and each projection step.

One trivial way to reduce clustering would be to damage the embedding in a way that universally lowers performance. We perform benchmarking to ensure we are not destroying large swathes of the embedding. We measure the results of unmodified, 2, 4 and 6 depth projections on the following word embedding benchmarks: Google Analogy [Mikolov et al., 2013], WS353 [Finkelstein et al., 2002], RG-65 [Rubenstein and Goodenough, 1965], MTurk-287 [Radinsky et al., 2012], MTurk-771 [Halawi et al., 2012], RW [Luong et al., 2013] and MEN [Bruni et al., 2012]. Results are summarized in Table 2. We observe that the model causes a modest loss in performance on similarity metrics across all projections. With the Google News set, while performing worse, the model was able to handle a larger amount of tasks due to its increased vocabulary. This combined with increased word density may explain the lower score.

We use these benchmarks only as an indicator of embedding integrity, not as a predictor for extrinsic evaluation downstream and not to suggest state-of-the-art results on the benchmarks. A similarly minor loss in accuracy is observed for embeddings modified by HARD-DEBIAS and GN-GloVe. This supports the notion that our projections selectively modify the targeted concept of interest and do not propagate to other learned patterns in the embedding.

Table 2: Results on  $D_4$  projected embeddings compared to original embeddings on benchmark datasets. Performance is measured in accuracy for word analogy tasks and in Spearman rank correlation for word similarity tasks. Number of projections performed with  $D_4$  are indicated.

Embedding	Analogy Google	Similarity					
		WS353	RG-65	MTurk-287	MTurk-771	RW	MEN
w2vnews	0.755	0.688	0.777	0.696	0.674	0.655	0.774
$D_4 = 2$	0.752	0.686	0.771	0.696	0.674	0.654	0.773
$D_4 = 4$	0.750	0.682	0.768	0.699	0.672	0.653	0.770
$D_4 = 6$	0.751	0.682	0.771	0.696	0.669	0.650	0.772
Google News	0.740	0.694	0.761	0.684	0.671	0.534	0.771
$D_4 = 2$	0.740	0.693	0.764	0.682	0.670	0.534	0.770
$D_4 = 4$	0.736	0.690	0.765	0.685	0.670	0.534	0.769
$D_4 = 6$	0.734	0.689	0.768	0.689	0.669	0.535	0.767

A criticism of de-biasing methods made by GG is that the number of male-biased professions cluster nearest the same male professions even after de-biasing. Conversely, feminine-biased professions such as nurse do not have as many male neighbors. We take the list of all professions that have a positive dot product with the gender direction and use this as our male profession label. We measure the nearest 100 neighbours for all words in the profession set provided in HARD-DEBIAS and count the number of male professions in the nearest neighbour results. Visual clustering of the sets before and after de-biasing is plotted in Figure 3. Attention should be drawn to the vectors at the most extreme

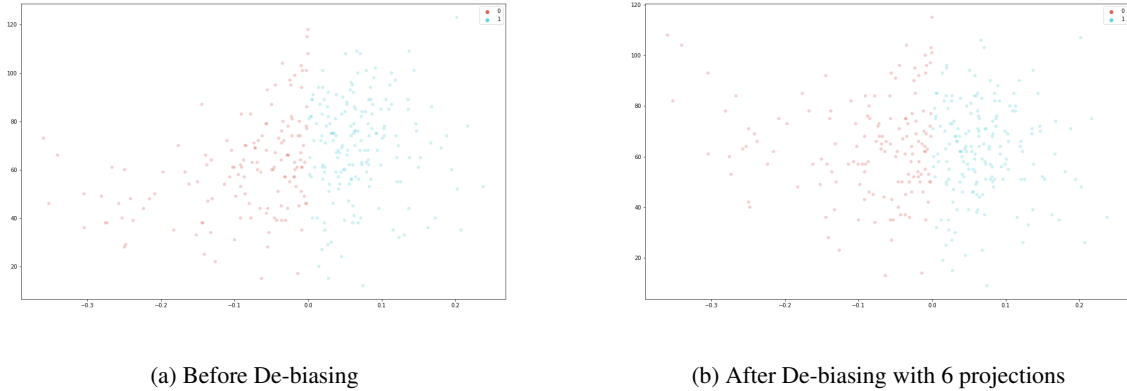


Figure 3: X-Axis shows the spread of selected profession word vector’s magnitude along the Gender Direction. Y-Axis shows the number of vectors in the nearest 100 set that are male-gendered. Points are coloured by gender (female → red, male → blue).

left in Figure 3. While much of the structure near the ‘0’ of the gender direction is maintained, the feminine oriented vectors show a marked increase in the number of neighbours that are male professions.

We are unable to reproduce the 0.747 Pearson correlation from GG for the gender direction to neighbour count, likely owing to us assigning different professions to gender, or using different thresholds along the gender direction. Measuring the Pearson correlation coefficient on our labels produces a result of 0.310 with a p-value of 1.5e-08. We apply our de-biasing technique with 6 projections and repeat the process with the de-biased vector set. Clustering on our de-biased set causes us to fail to reject the null hypothesis (p=0.226). As our goal was to remove a significant correlation between the two, we interpret this as a successful result. Thus, it appears that  $D_4$  projections cause a significant change in the coefficient.

The final de-biasing experiment we conducted from GG was to measure the ability of a radial basis function SVM to recover word structure. We use default parameters and achieve a model accuracy of 59.1%, which is the same score that our linear SVM converged to when applying  $D_4$ . Running the same test on the Google News embedding has a result of 51.5%. This shows a marked improvement over the scores of 88.88% from HARD-DEBIAS and 96.53% from GN-GloVe documented by GG.

In this work we do not attempt to maintain analogies such as Man - Waiter = Woman - Waitress. We anticipate applications of this technique in settings where any notion of gender is undesirable in the final system that the word embedding will be applied to. However, we note that while the gender information is gone from  $X_{\perp}$ , it is retained in  $X_{\parallel}$ ; therefore, if retaining gender structure is required for some tasks, including dimensions of  $X_{\parallel}$  is straightforward.

## 4 Relationship to Other Methods

Below, we discuss how  $D_4$  relates to two methods: adversarial training and PCA.

The term “adversarial” in machine learning has had two major uses; one use describes settings where noise is imagined to be introduced into training data by an entity that is actively trying to hinder learning (see e.g. Biggio et al. [2011].) More recently, it has been applied to neural network training that seeks to construct a feature representation that is able to learn a target concept but is also *unable* to learn a distractor concept [Goodfellow et al., 2014]. This is undertaken during learning of the representation, where the two types of training are interleaved. The goal is similar to that of  $D_4$  but functionally has some important differences:  $D_4$  creates a representation space orthogonal to the decision direction learned from the specified target. The resulting new representation should perform poorly on the specified target, but there is no specification of a particular learning task that the representation should perform well on. Second, adversarial training can create different nonlinear representations depending on network architecture, whereas  $D_4$  operates only in the linear (or possibly kernel) feature space. Finally,  $D_4$  can be applied as a post-processing step that is computationally inexpensive relative to training a large neural network.

Like  $D_4$ , Principal Component Analysis (PCA) and its variants [Jolliffe and Cadima, 2016] project the *columns* of the data matrix onto a lower-dimensional space with an orthogonal representation. The goal of such methods is to preserve as much of the structure of the matrix as possible in the squared-error sense. Iterative methods for PCA, such

as Schur-complement deflation, sequentially identify directions onto which the columns of the data matrix are projected. We may consider what happens if instead of projecting the rows of  $\mathbf{X}$  onto the space orthogonal to  $\omega$ , we project the columns of  $\mathbf{X}$  onto the space orthogonal to  $\mathbf{X}\omega$  using Schur-complement deflation. We have the following:

**Theorem 1.** *If  $\mathbf{X}$  has full rank, then Schur-complement deflation of the columns of  $\mathbf{X}$  onto the orthogonal complement of  $\mathbf{X}\omega$  and decision-direction deflation onto the orthogonal complement of  $\omega$  are equivalent if and only if the columns of  $\mathbf{X}$  are orthonormal.*

*Proof.* Note that  $\left(\mathbf{I} - \frac{\mathbf{X}\omega\omega^\top\mathbf{X}^\top}{\omega^\top\mathbf{X}^\top\mathbf{X}\omega}\right)\mathbf{X} = \mathbf{X}\left(\mathbf{I} - \omega\omega^\top\frac{\mathbf{X}^\top\mathbf{X}}{\omega^\top\mathbf{X}^\top\mathbf{X}\omega}\right)$ . If  $\mathbf{X}$  has orthonormal columns, then  $\mathbf{X}^\top\mathbf{X} = \mathbf{I}$  and the last expression simplifies to projecting the rows of  $\mathbf{X}$  onto the orthogonal complement of  $\omega$ . In the other direction, if the Schur-complement deflation is equivalent to projection onto the orthogonal complement of  $\omega$ , then we have  $\omega\omega^\top\frac{\mathbf{X}^\top\mathbf{X}}{\omega^\top\mathbf{X}^\top\mathbf{X}\omega} = \omega\omega^\top$ . This would imply that  $\frac{\mathbf{X}^\top\mathbf{X}}{\omega^\top\mathbf{X}^\top\mathbf{X}\omega}$  is idempotent. If  $\mathbf{X}$  has full rank, then  $\mathbf{X}^\top\mathbf{X} = \mathbf{I}$  since the identity is the only full-rank idempotent matrix.  $\square$

The interesting implication of Theorem 1 is that if the features in  $\mathbf{X}$  are *not* orthogonal, then the two projections give different results. In particular, this means that projecting the columns of  $\mathbf{X}$  onto the orthogonal complement of  $\mathbf{X}\omega$  will not in general remove all variability in the direction of  $\omega$ , regardless of the method used to find  $\omega$ .

## 5 Conclusion

We have described a new algorithm, Decision-Directed Data Decomposition, for removing information from a dataset. It is simple and scalable, and provides state-of-the-art results in word embedding de-biasing. We have also shown that it has promise as an alternative to adversarial training.

For future work, we are interested in two approaches for mitigating the loss of information by the  $D_4$  process. The first is to explicitly generate a larger set of non-linear features, for example random Fourier features [Rahimi and Recht, 2008] approximating the radial basis function kernel, and then apply linear projections to this expanded set to remove undesirable information. Another is to employ the kernel version of  $D_4$  described in the supplemental material directly; however this may not be feasible for large  $n$  since it assumes a full kernel matrix. Therefore we aim to develop approaches that will use only sparse subset of the kernel matrix, much like sequential minimal optimization [Platt, 1998], to reduce computational cost in this case.

## References

- B. Biggio, B. Nelson, and P. Laskov. Support Vector Machines Under Adversarial Label Noise. Technical report, 2011. URL <http://proceedings.mlr.press/v20/biggio11/biggio11.pdf>.
- B. Biggio, I. Corona, B. Nelson, B. I. P. Rubinstein, D. Maiorca, G. Fumera, G. Giacinto, and F. Roli. *Security Evaluation of Support Vector Machines in Adversarial Environments*, pages 105–153. Springer International Publishing, Cham, 2014. ISBN 978-3-319-02300-7. doi: 10.1007/978-3-319-02300-7\_4. URL [https://doi.org/10.1007/978-3-319-02300-7\\_4](https://doi.org/10.1007/978-3-319-02300-7_4).
- T. Bolukbasi, K.-W. Chang, J. Zou, V. Saligrama, and A. Kalai. Man is to Computer Programmer as Woman is to Homemaker? Debiasing Word Embeddings. jul 2016. URL <http://arxiv.org/abs/1607.06520>.
- E. Bruni, G. Boleda, M. Baroni, and N.-K. Tran. Distributional Semantics in Technicolor. Technical report, 2012. URL <http://www.vlfeat.org/>.
- A. Caliskan, J. J. Bryson, and A. Narayanan. Semantics derived automatically from language corpora contain human-like biases. *Science (New York, N.Y.)*, 356(6334):183–186, apr 2017. ISSN 1095-9203. doi: 10.1126/science.aal4230. URL <http://www.ncbi.nlm.nih.gov/pubmed/28408601>.
- X. Dai, M. Bikdash, and B. Meyer. From social media to public health surveillance: Word embedding based clustering method for twitter classification. In *SoutheastCon 2017*, pages 1–7. IEEE, mar 2017. ISBN 978-1-5386-1539-3. doi: 10.1109/SECON.2017.7925400. URL <http://ieeexplore.ieee.org/document/7925400/>.
- L. Finkelstein, E. Gabrilovich, Y. Matias, E. Rivlin, Z. Solan, G. Wolfman, and E. Ruppin. Placing search in context: the concept revisited. *ACM Transactions on Information Systems*, 20(1):116–131, jan 2002. ISSN 10468188. doi: 10.1145/503104.503110. URL <http://portal.acm.org/citation.cfm?doid=503104.503110>.
- L. A. Gatys, A. S. Ecker, and M. Bethge. Image Style Transfer Using Convolutional Neural Networks. Technical report, 2016. URL [http://openaccess.thecvf.com/content/{}\\_cvpr/{}\\_2016/papers/Gatys/{}\\_Image/{}\\_Style/{}\\_Transfer/{}\\_CVPR/{}\\_2016/{}\\_paper.pdf](http://openaccess.thecvf.com/content/{}_cvpr/{}_2016/papers/Gatys/{}_Image/{}_Style/{}_Transfer/{}_CVPR/{}_2016/{}_paper.pdf).



- H. Gonen and Y. Goldberg. Lipstick on a pig: Debiasing methods cover up systematic gender biases in word embeddings but do not remove them. In *Proceedings of the 2019 Conference of the North American Chapter of the Association for Computational Linguistics: Human Language Technologies, Volume 1 (Long and Short Papers)*, pages 609–614, 2019.
- I. J. Goodfellow, J. Pouget-Abadie, M. Mirza, B. Xu, D. Warde-Farley, S. Ozair, A. Courville, and Y. Bengio. Generative Adversarial Nets. Technical report, 2014. URL <http://www.github.com/goodfeli/adversarial>.
- G. Halawi, G. Dror, E. Gabrilovich, and Y. Koren. Large-scale learning of word relatedness with constraints. In *Proceedings of the 18th ACM SIGKDD international conference on Knowledge discovery and data mining - KDD '12*, page 1406, New York, New York, USA, 2012. ACM Press. ISBN 9781450314626. doi: 10.1145/2339530.2339751. URL <http://dl.acm.org/citation.cfm?doid=2339530.2339751>.
- I. T. Jolliffe and J. Cadima. Principal component analysis: a review and recent developments. *Philosophical Transactions of the Royal Society A: Mathematical, Physical and Engineering Sciences*, 374(2065):20150202, 2016.
- E. Jones, T. Oliphant, and P. Peterson. {SciPy}: Open source scientific tools for {Python}. 2014.
- T. Luong, R. Socher, and C. D. Manning. Better Word Representations with Recursive Neural Networks for Morphology. *undefined*, 2013. URL <https://www.semanticscholar.org/paper/Better-Word-Representations-with-Recursive-Neural-Luong-Socher/00a28138c74869cfb8236a18a4dbe3a896f7a812>.
- T. Mikolov, K. Chen, G. Corrado, and J. Dean. Efficient Estimation of Word Representations in Vector Space. jan 2013. URL <http://arxiv.org/abs/1301.3781>.
- F. Pedregosa, G. Varoquaux, A. Gramfort, V. Michel, B. Thirion, O. Grisel, M. Blondel, P. Prettenhofer, R. Weiss, V. Dubourg, J. Vanderplas, A. Passos, D. Cournapeau, M. Brucher, M. Perrot, and É. Duchesnay. Scikit-learn: Machine Learning in Python. *Journal of Machine Learning Research*, 12(Oct):2825–2830, 2011. ISSN ISSN 1533-7928. URL <http://jmlr.csail.mit.edu/papers/v12/pedregosa11a.html>.
- J. Platt. Sequential minimal optimization: A fast algorithm for training support vector machines. 1998.
- K. Radinsky, E. Agichtein, E. Gabrilovich, and S. Markovitch. *A Word at a Time: Computing Word Relatedness using Temporal Semantic Analysis*. 2012. ISBN 9781450306324. URL <https://citeseerx.ist.psu.edu/viewdoc/download?doi=10.1.1.205.8607&rep=rep1&type=pdf>.
- A. Rahimi and B. Recht. Random features for large-scale kernel machines. In *Advances in neural information processing systems*, pages 1177–1184, 2008.
- B. Recht, R. Roelofs, L. Schmidt, and V. Shankar. Do ImageNet Classifiers Generalize to ImageNet? feb 2019. URL <http://arxiv.org/abs/1902.10811>.
- M. T. Ribeiro, S. Singh, and C. Guestrin. "Why Should I Trust You?": Explaining the Predictions of Any Classifier. feb 2016. URL <http://arxiv.org/abs/1602.04938>.
- A. Rosenberg and J. Hirschberg. V-Measure: A conditional entropy-based external cluster evaluation measure. Technical report, 2007. URL <https://www.aclweb.org/anthology/D07-1043>.
- H. Rubenstein and J. B. Goodenough. Contextual correlates of synonymy. *Communications of the ACM*, 8(10):627–633, oct 1965. ISSN 00010782. doi: 10.1145/365628.365657. URL <http://portal.acm.org/citation.cfm?doid=365628.365657>.
- K. Simonyan and A. Zisserman. Very Deep Convolutional Networks for Large-Scale Image Recognition. sep 2014. URL <http://arxiv.org/abs/1409.1556>.
- R. C. Team et al. R: A language and environment for statistical computing. 2013.
- L. Van Der Maaten and G. Hinton. Visualizing Data using t-SNE. Technical report, 2008. URL [https://lvdmaaten.github.io/publications/papers/JMLR\\_{\\_}2008.pdf](https://lvdmaaten.github.io/publications/papers/JMLR_{_}2008.pdf).
- J. Zhao, Y. Zhou, Z. Li, W. Wang, and K.-W. Chang. Learning Gender-Neutral Word Embeddings. Technical report, 2018. URL [https://github.com/uclanlp/gn\\_glove](https://github.com/uclanlp/gn_glove).